Electronic Supplementary Material (ESI) for ChemComm.

Nitrogen-Doped Carbon Nanosheet Composited Platinum-Cobalt Single Atom Alloy Catalyst for Effective Hydrogen Evolution Reaction

Xudong Niu,‡ Huilong Geng,‡ Zhengyu Lv, Jian Wei,* Dongyao Xu* and Wenxing Chen*

Chemicals.

Chloroplatinic acid hexahydrate ($H_2PtCl_6·6H_2O$, Aladdin), Cobalt nitrate hexahydrate ($Co(NO_3)_2·6H_2O$, Aladdin), dicyandiamide (DCDA, AR, Macklin), trimesic acid (99%, Innochem,), Nafion D-521 dispersion (5% w/w in water and 1-propanol) (Alfa Aesar), analytical grade anhydrous methanol and ethanol (Sinopharm Chemical), H_2SO_4 (analytical grade, Sinopharm Chemical), Deionized water was prepared with ultra-pure water system. All the chemicals were analytical grade and used without further purification.

Synthesis.

Preparation of PtCo SAA/NC Catalyst

Firstly, Chloroplatinic acid hexahydrate ($H_2PtCl_6·6H_2O$) and cobalt nitrate hexahydrate ($Co(NO_3)_2·6H_2O$) act as metal precursors, dicyan-diamide (DCDA) and trimesic acid act as N and C sources, which act as hosts to capture Co and Pt. These raw materials are uniformly mixed in one step, and then pyrolysis is performed in N_2 at high temperature, anchoring the Co and Pt sites onto nitrogen-doped carbon (NC).

Typically, 2 g DCDA and 0.2 g trimesic acid were dissolved in 10 mL deionized water, 15 mg $Co(NO_3)_2·6H_2O$ and 3mg $H_2PtCl_6·6H_2O$ were also added to the solution. Then the mixed solution was placed in a rotary evaporator at 50 ºC and adjust to the appropriate speed and stop when the solvent evaporates. Subsequently, the dried product was ground into powder and placed in a porcelain boat in a tube furnace. The boat was annealed at 800 ℃ under the N_2 atmosphere for 2 h with a ramping rate of 5 ℃/min, then cooled down to room temperature. The prepared PtCo SAA/NC was washed thoroughly with ethanol and deionized water. Finally, the samples were dried in vacuum at 60 ºC for overnight.

Preparation of Co NPs/NC Catalyst

DCDA (1 g) and trimesic acid (0.1 g) were dissolved in 5 mL deionized water, while 10 mg $Co(NO_3)_2·6H_2O$ were also added to the solution. Then the mixed solution was placed in a rotary evaporator at 50 ºC and adjust to the appropriate speed and stop when the solvent evaporates. Subsequently, the dried product was ground into powder and placed in a porcelain boat in a tube furnace. The boat was annealed at 800 ℃ under the N_2 atmosphere for 2 h with a ramping rate of 5 ℃/min, then cooled down to room temperature. The prepared Co NPs/NC was washed thoroughly with ethanol and deionized water. Finally, the samples were dried in vacuum at 60 ºC for overnight.

Preparation of NC

DCDA (1 g) and trimesic acid (0.1 g) were ground and mixed evenly. The mixed powder was put into a porcelain boat in a tube furnace. The boat was annealed at 800 ℃ under the N_2 atmosphere for 2 h with a ramping rate of 5 ℃/min, then cooled down to room temperature. The prepared NC was washed thoroughly with ethanol and deionized water. Finally, the samples were dried in vacuum at 60 ℃ for overnight.

Characterization.

Through a transmission electron microscope (TEM, JEOL JEM-2100F microscope, 200 kV) and a scanning electron microscope (SEM, JSM-6700F, 5 kV), the morphologies of samples were characterized. High resolution transmission electron microscope (HRTEM) was performed by FEI Tecnai G2 F20 S-Twin with the 200 kV operating voltage and collected the elemental mappings with the assistance of X-ray energy dispersive spectroscopy detector. The X-ray powder diffraction (XRD) patterns of the samples were tested by X-ray powder diffraction (XRD, RigakuTTR-III X-ray diffractometer with Cu Kα radiation, λ =1.5418 Å). The atomic-resolution HAADF-STEM characterization was conducted using a probe aberration-corrected microscope, JEOL JEM-ARM200F equipped with cold emitter, an accelerating voltage of 200kV. X-ray photoelectron spectroscopy (XPS) was obtained by PerkinElmer Physics PHI 5300 energy spectrometer using mono-chromatic Al Kα radiation (1486.7 eV). At beamline BL12B of the National Synchrotron Radiation Laboratory (NSRL) of China, the X-ray absorption near-edge structure (XANES) spectra were tested.

XAFS measurements and analysis

The acquired EXAFS data were processed according to the standard procedures by using the ATHENA module of the IFEFFIT software packages. The detailed fitting process is stated below:

The obtained EXAFS spectra underwent the subtraction of post-edge background from the overall absorption and then normalization with respect to the edge-jump step. Subsequently, the χ(k) data were Fourier transformed to real (R) space by using a hanning windows (dk=1.0 $Å^{-1}$) to separate the EXAFS contributions from different coordination shells. To obtain the quantitative structural parameters around central atoms, least-squares curve parameter fitting was conducted by using the ARTEMIS module of the IFEFFIT software packages.

The following EXAFS equation was used:

$$\chi(k)=\sum_j \frac{N_j S_o^2 F_j(k)}{k R_j^2}\exp[-2k^2\sigma_j^2]\exp[\frac{-2R_j}{\lambda(k)}]\sin[2kR_j+\phi_j(k)]$$

In the equation, S_0^2 represent the amplitude reduction factor, $F_j(k)$ is the effective curved-wave backscattering amplitude, N_j is the number of neighbors in the j^{th} atomic shell, R_j represent the distance between the X-ray absorbing central atom and the atoms in the j^{th} atomic shell (backscatterer), λ represent the mean free path in Å, σ_j is the Debye-Waller parameter of the j^{th} atomic shell (variation of distances around the average R_j) and $\phi_j(k)$ is the phase shift (including the phase shift for each shell and the total central atom phase shift). The functions $F_j(k)$, λ and $\phi_j(k)$ were calculated with the ab initio code FEFF8.2

The coordination numbers of model samples (Ni foil) were fixed as the nominal values. The obtained S_0^2 was fixed in the subsequent fitting of PtCo SAA/NC sample. While the internal atomic distances R, Debye-Waller factor σ^2, and the edge-energy shift ΔE_0 were allowed to run freely.

Electrochemical Measurements.

The electrochemical measurements were carried out on a CHI 660e electrochemical workstation in a three-electrode configuration cell using as-prepared electrode as the working electrode, graphite rod as the counter electrode, and Ag/AgCl (saturated KCl) as the reference electrode in 0.5 M H_2SO_4 aqueous electrolyte. To prepare a homogeneous ink, 4 mg of the sample and 10 μL of a 5 wt% Nafion solution were dispersed in 1 mL of a water-isopropanol solution with a 1:1 volume ratio, followed by 30 min sonication. Then 20 μL of the dispersion (containing 80 μg of catalyst) wasloaded onto a glassy carbon electrode (5 mm in diameter, catalyst loading 0.408 mg cm^{-2}). The commercial 20 wt% Pt/C electrode was prepared using the same procedure for comparison. The LSV curves were conducted at scan rate of 20 mV/s. All of the potentials were quoted against a reversible hydrogen electrode (RHE).

Density functional theory (DFT) calculation.

All the calculations were carried out with density functional theory (DFT) method as implemented in the Vienna Ab Initio Simulation Package (VASP). We use the projected augmented wave (PAW) potentials to simulate the interaction between valence electrons and nuclei. In addition, Perdew-BurkeErnzerh (PBE) and Generalized Gradient Approximation (GGA) using exchange correlation functions are used to study electron transfer and interrelationships. The kinetic energy cut-off was set at 500 eV,

the total energies were converged to 1×10^{-5} eV, the convergence criterion for the residual forces on the atoms was set to 0.05 eV $Å^{-1}$ during the relaxation. A $5 \times 5 \times 1$ k-mesh was employed for the Brillouin zone integrations. Hydrogen adsorption energies were calculated relative to H_2 (g) as

$$\Delta E = E(slab + H) - E(slab) - \frac{1}{2}E(H_2) \#(1)$$

The associated hydrogen free energy is

$$\Delta G = \Delta E + \Delta ZPE - T\Delta S \#(2)$$

ΔE is the reaction energy of reactant and product species adsorbed on the catalyst directly obtained from DFT calculations; ΔZPE being the difference in zero-point energy and ΔS the difference in entropy between the adsorbed state and gas phase.

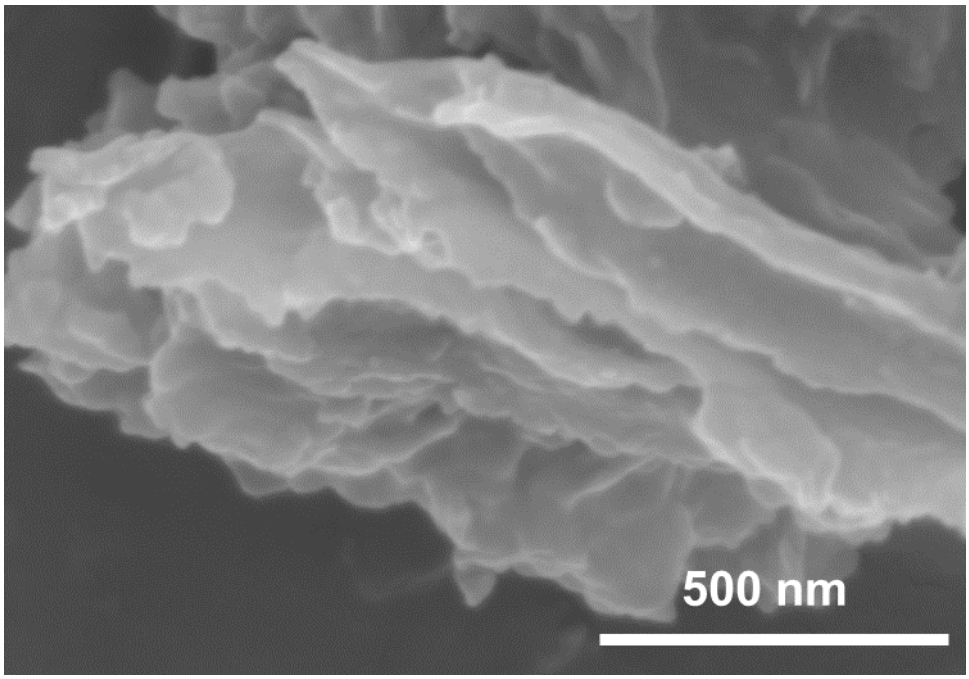

Figure S1. SEM image of PtCo SAA/NC.

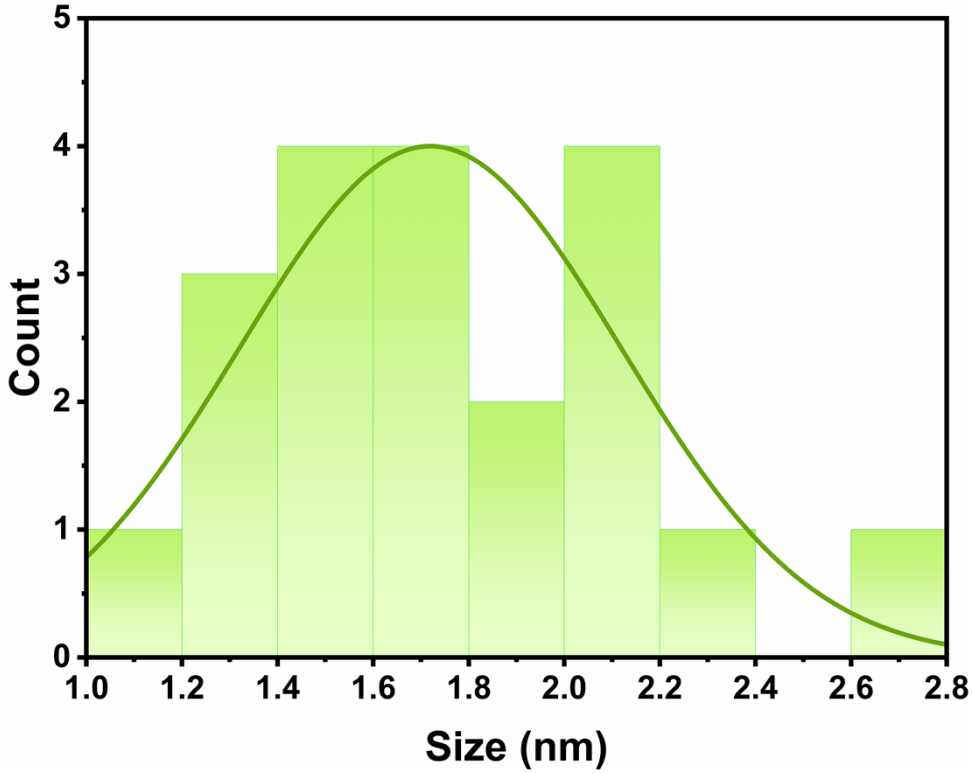

Figure S2. Size distribution of PtCo SAA particles.

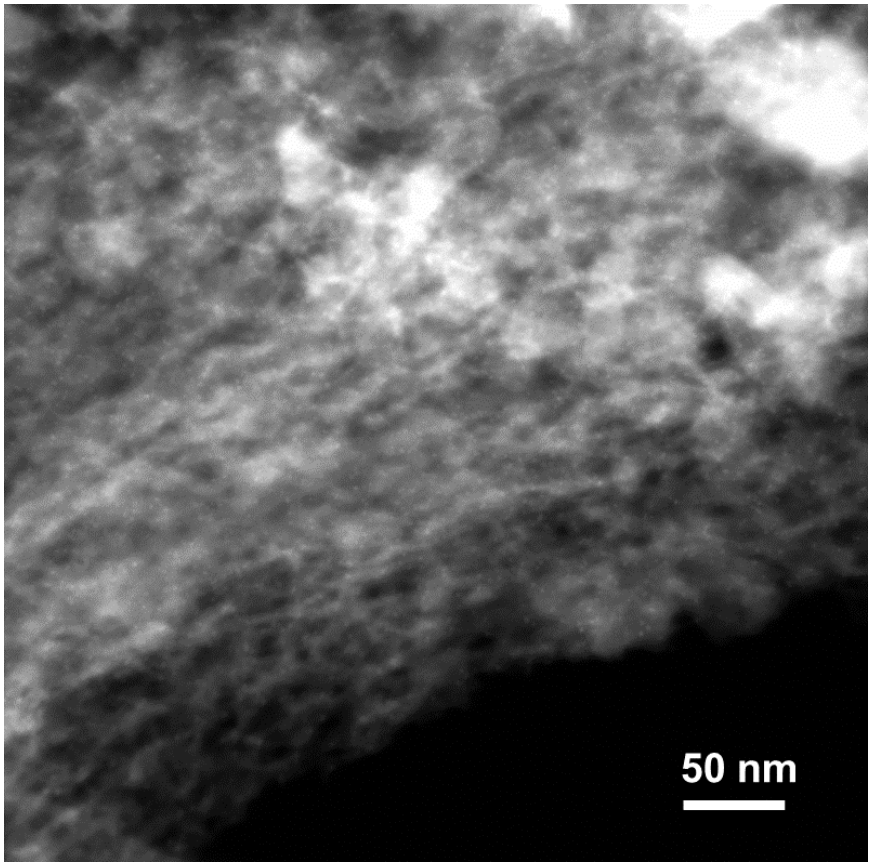

Figure S3. HAADF-STEM image of PtCo SAA/NC.

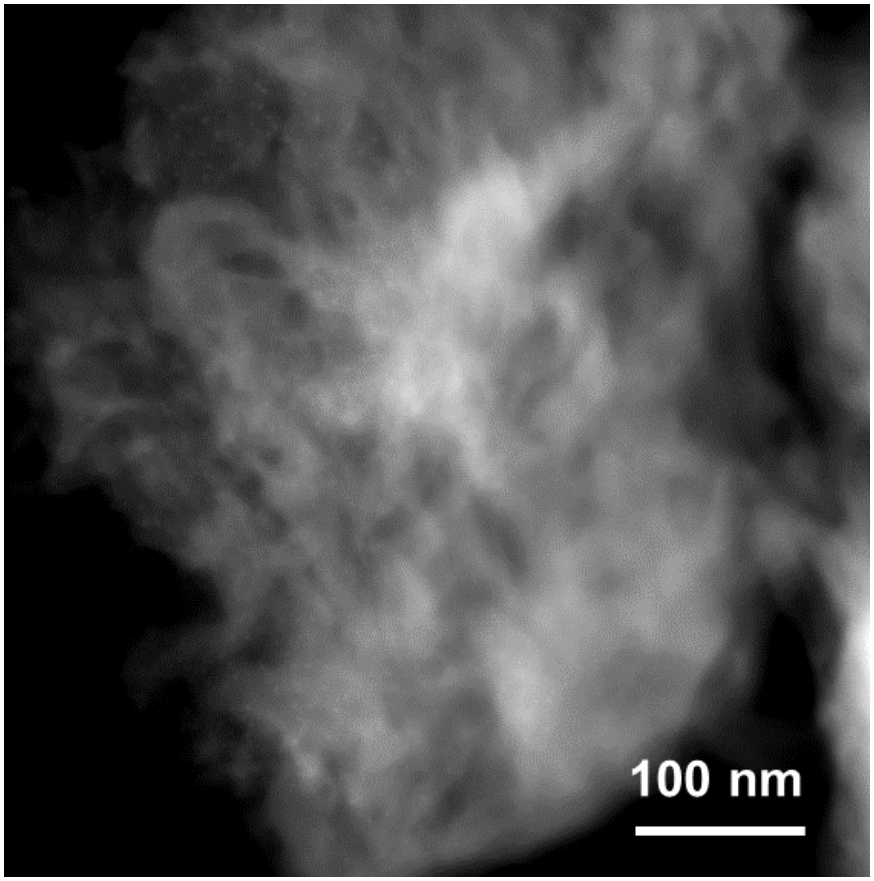

Figure S4. HAADF-STEM image of Co NPs/NC.

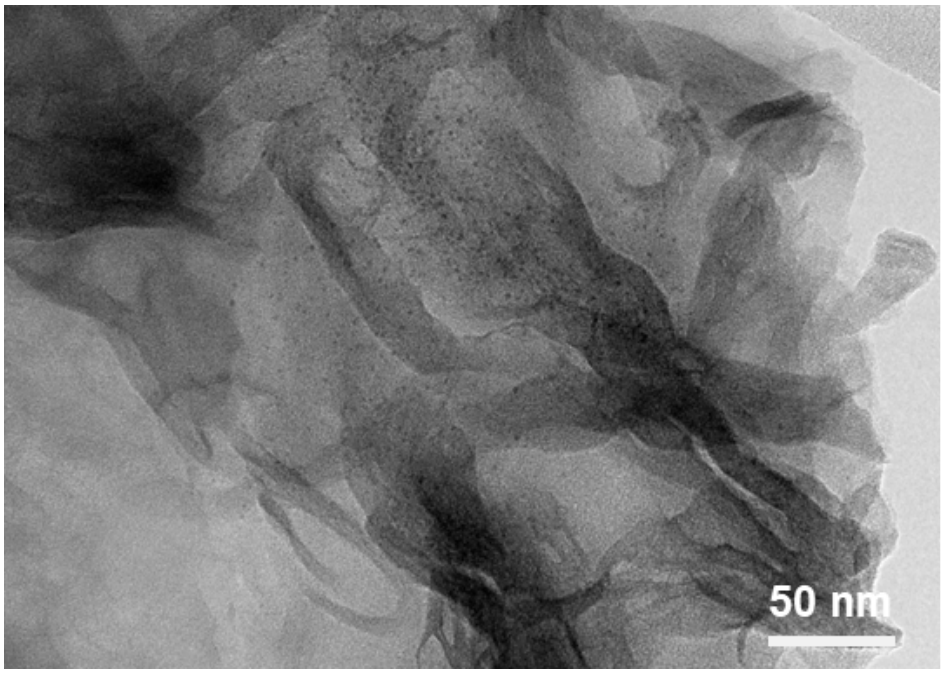

Figure S5. TEM image of Co NPs/NC.

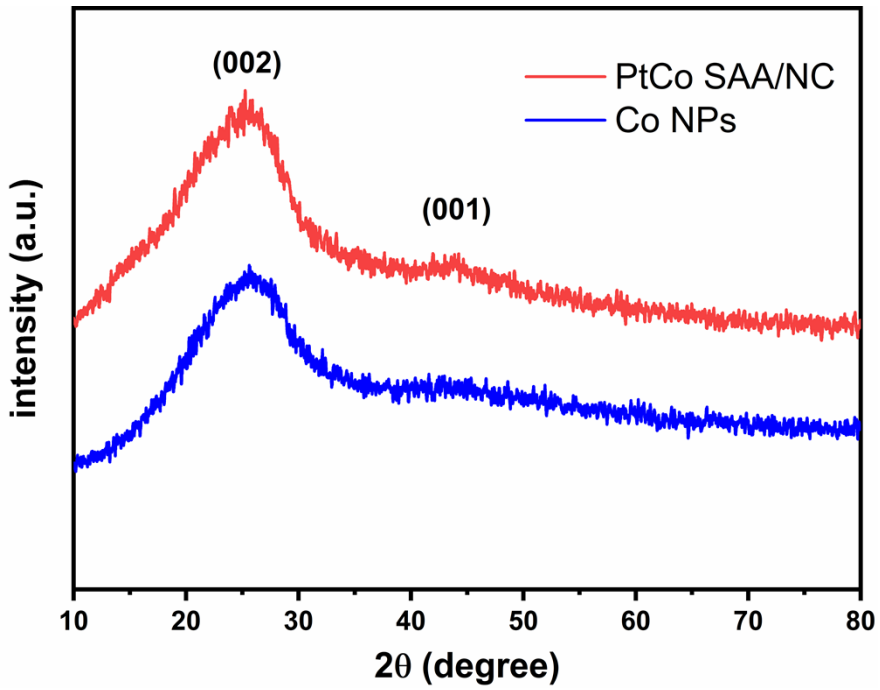

Figure S6. XRD pattern of PtCo SAA/NC and Co NPs/NC.

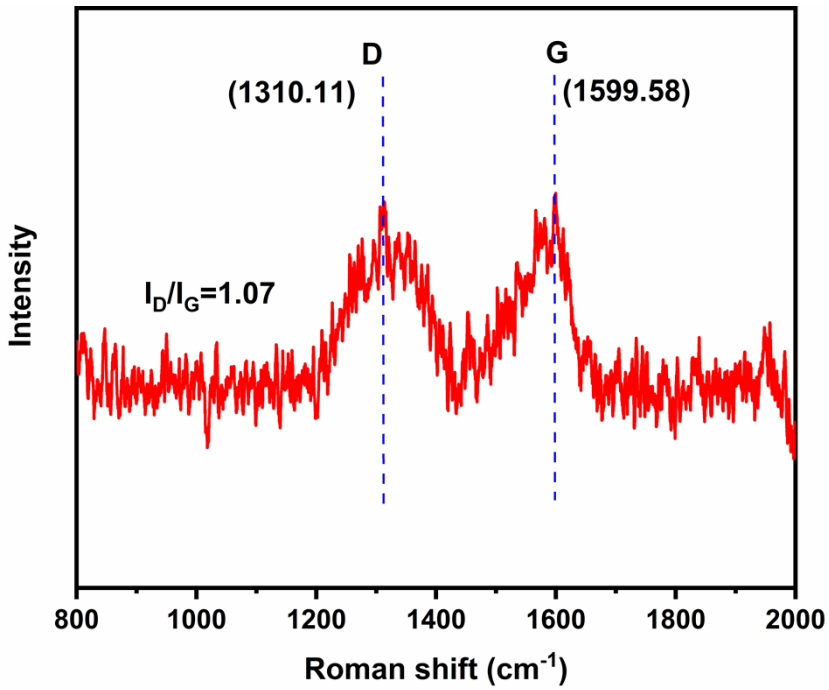

Figure S7. Raman spectroscopy of PtCo SAA/NC.

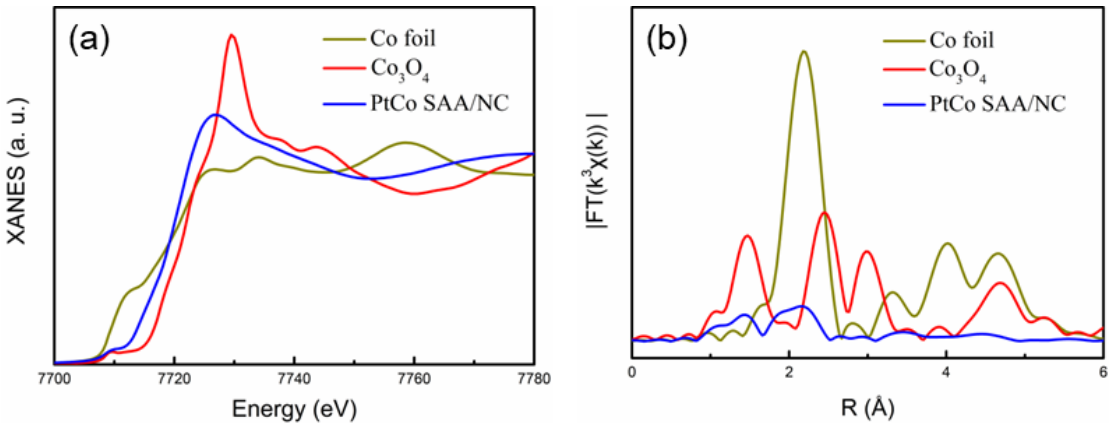

Figure S8. The experimental Co K-edge (a) XANES spectra and (b) EXAFS spectra of PtCo SAA/NC and counterparts.

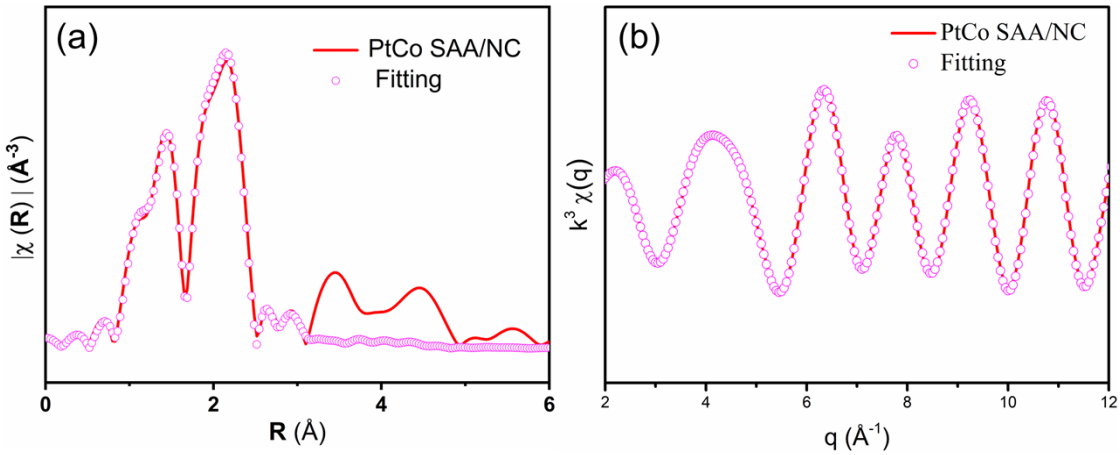

Figure S9. The EXAFS fitting results of PtCo SAA/NC at Co K-edge. (a) R and (b) q space.

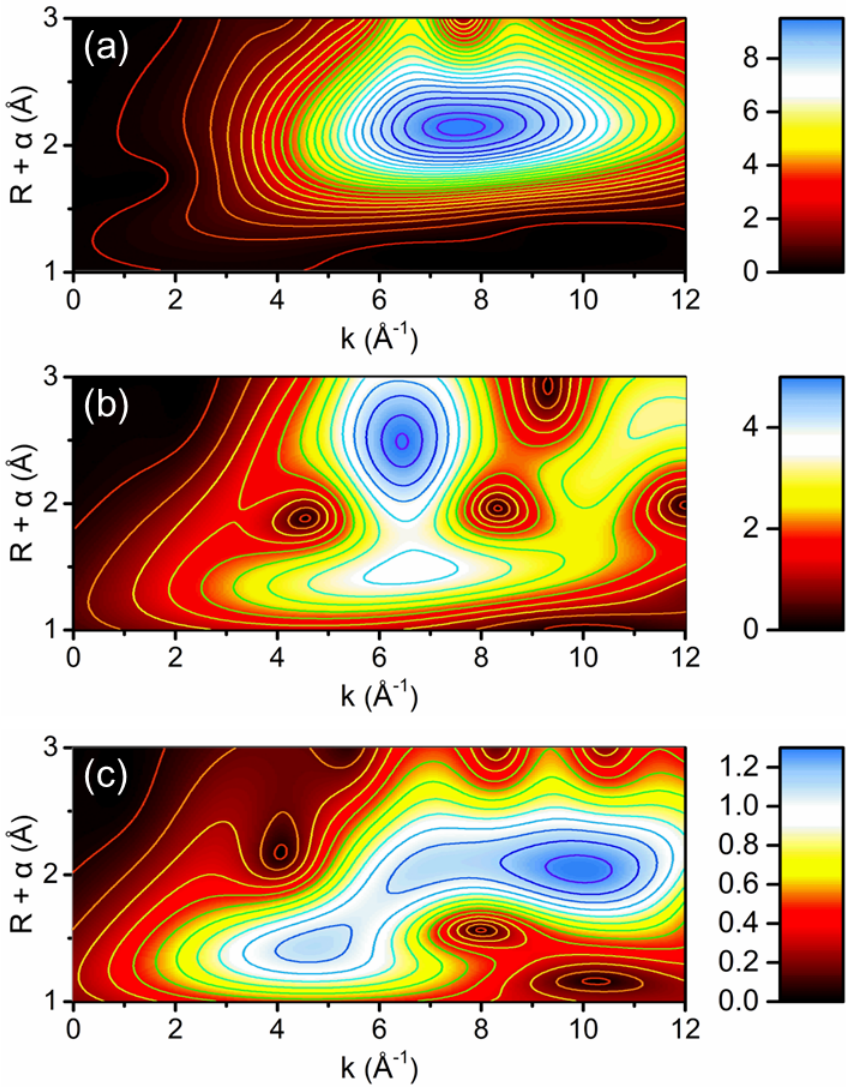

Figure S10. WT-EXAFS plots of (a) Co foil, (b) Co_3O_4, (c) PtCo SAA/NC.

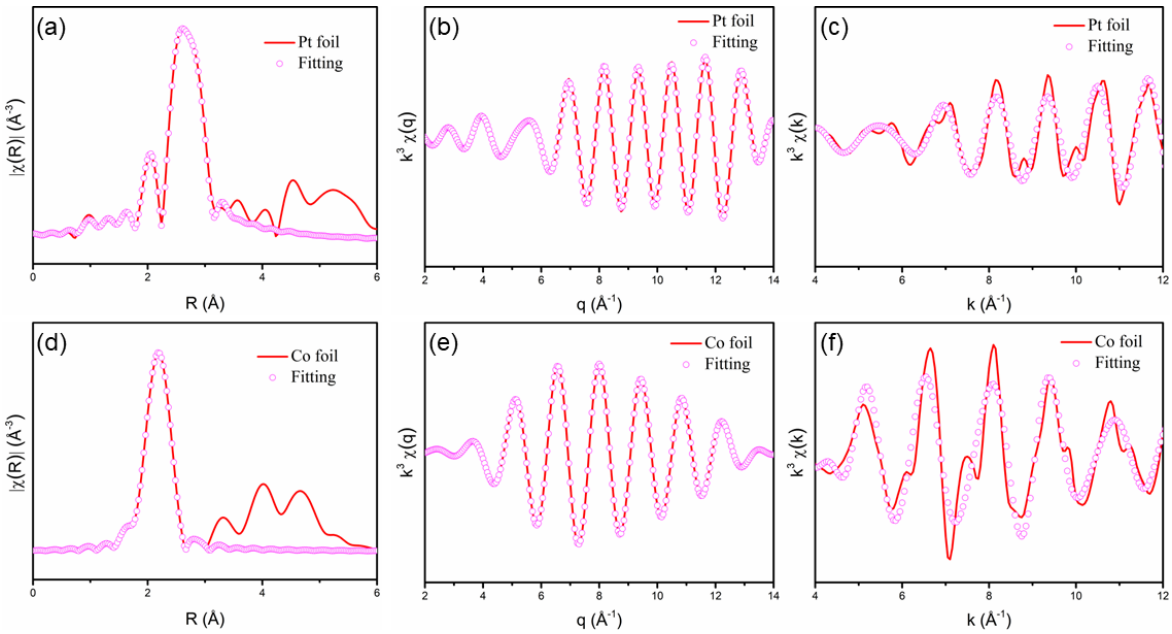

Figure S11. The EXAFS fitting results of Pt foil at (**a**) R, (**b**) q and (**c**) k space. The EXAFS fitting results of Co foil at (**d**) R, (**e**) q and (**f**) k space.

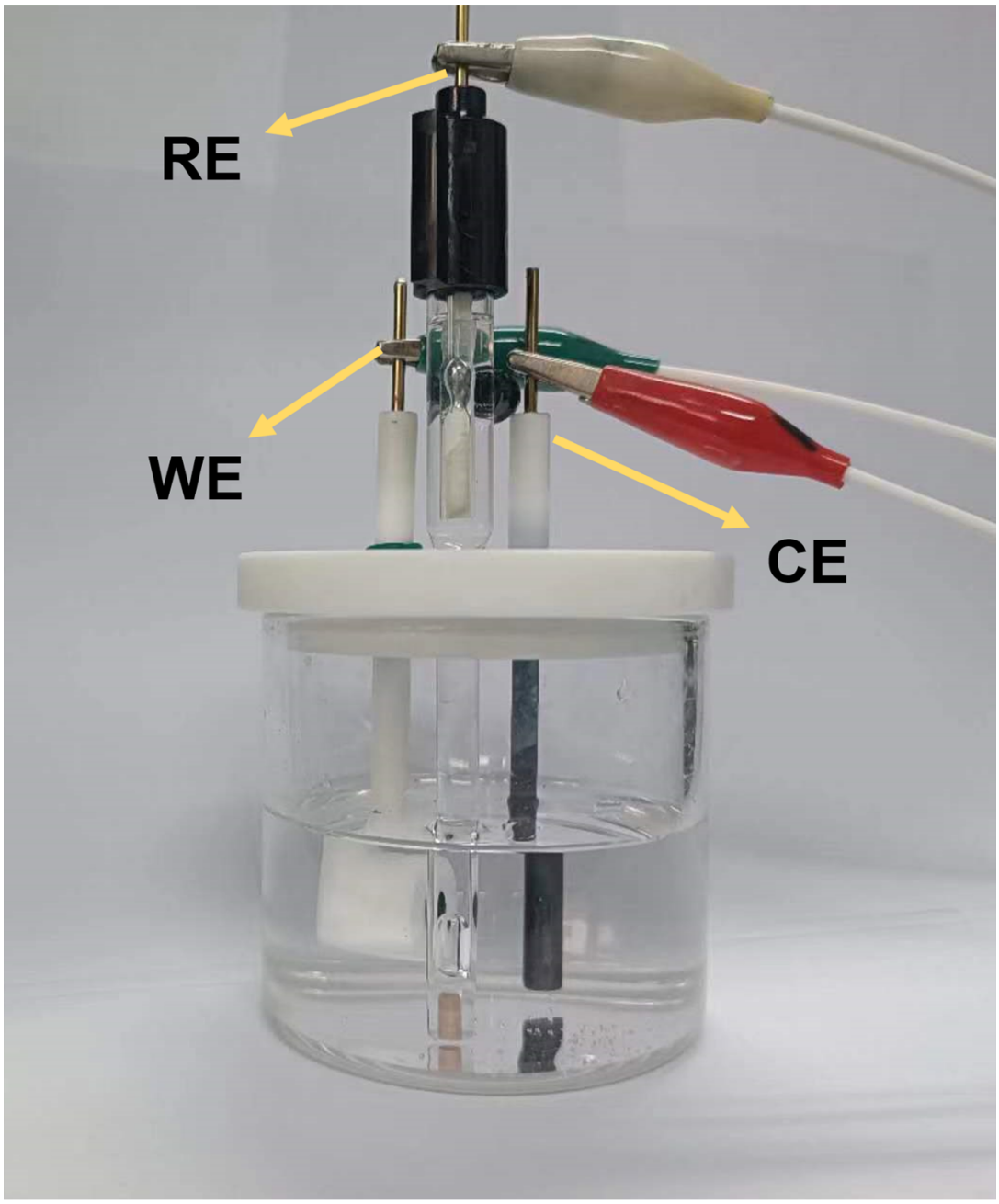

Figure S12. Photograph of the typical three-electrode setup for the electrochemical HER measurements. (The red electrode clamp is connected to the counter electrode, the white electrode clamp is connected to the reference electrode, and the green electrode clamp is connected to the working electrode)

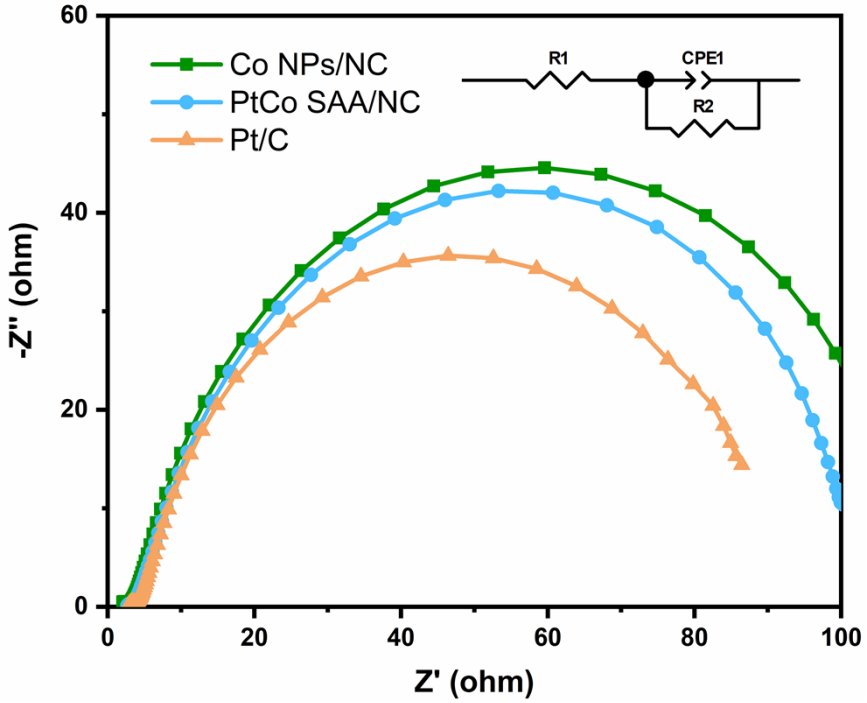

Figure S13. Nyquist plots of the PtCo SAA/NC, Co NPs/NC, and Pt/C at the overpotential of 50 mV.

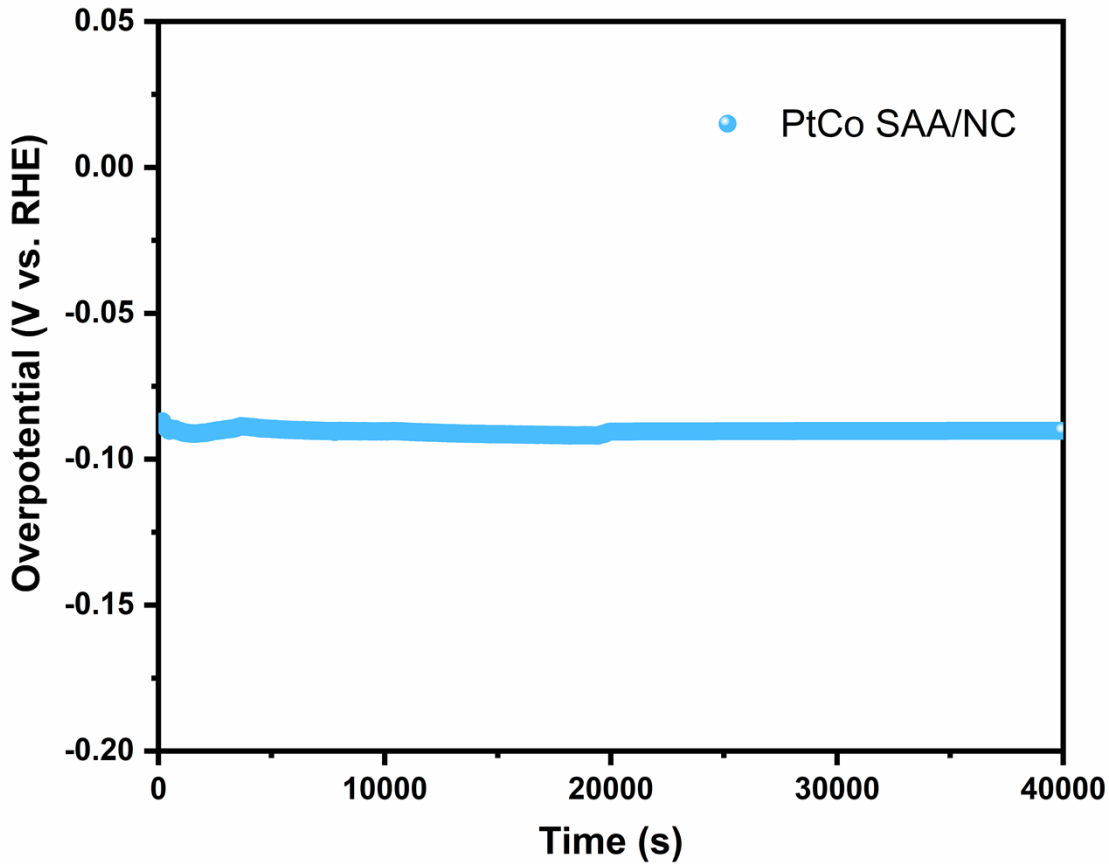

Figure S14. The chronopotentiometric measurement of PtCo SAA/NC at the current density of 10 mA cm^{-2} in acidic media.

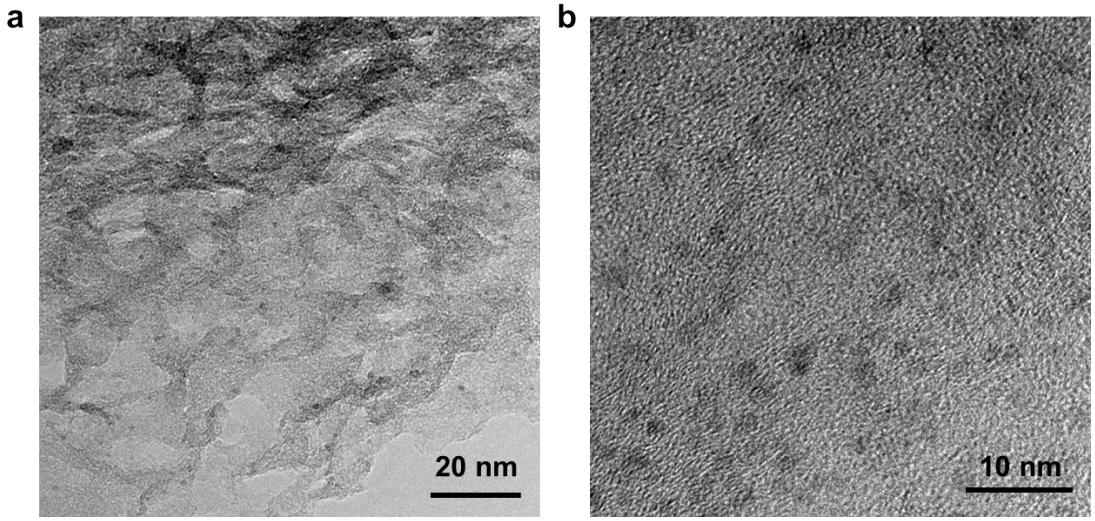

Figure S15. (a) TEM and (b) HRTEM images of PtCo SAA/NC after durability test.

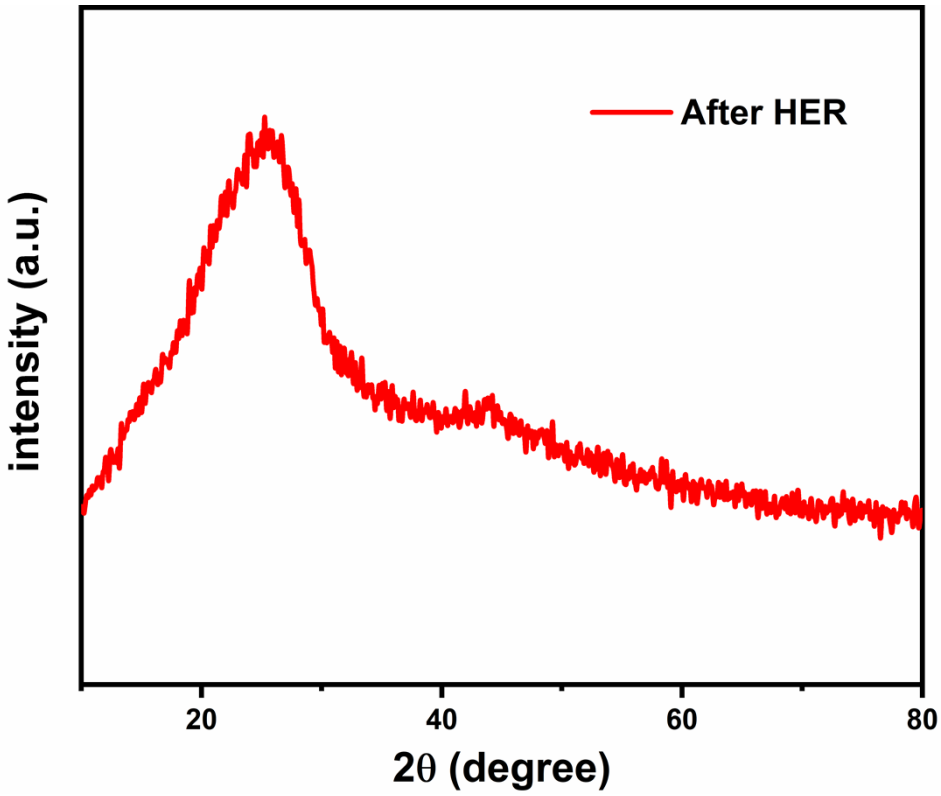

Figure S16. XRD pattern of the PtCo SAA/NC after durability test.

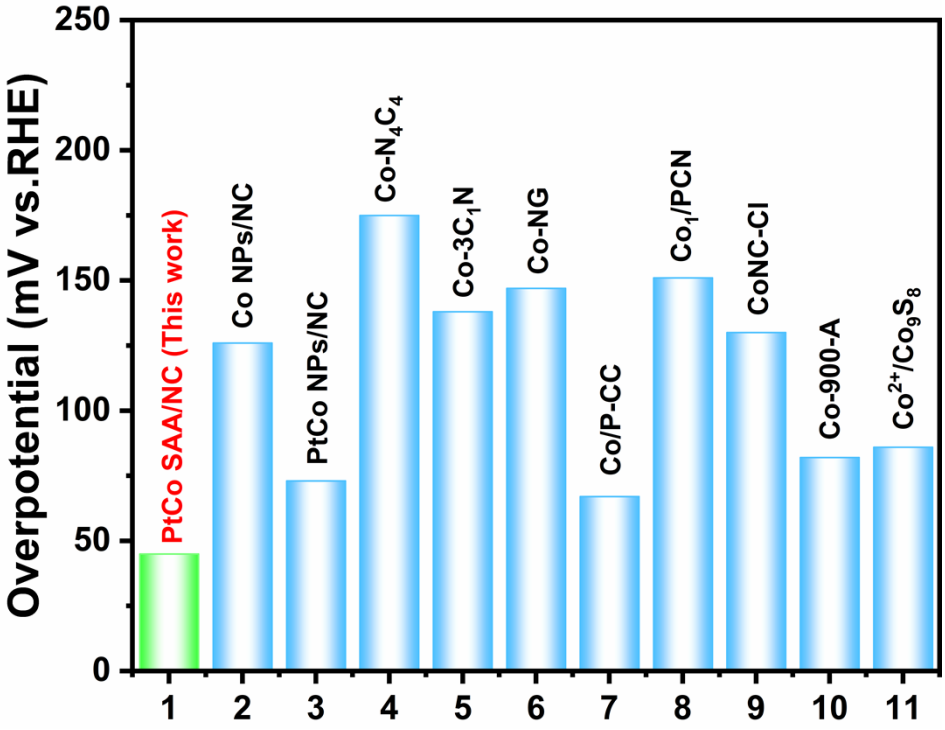

Figure S17. Overpotential at 10 mA cm^{-2} values of PtCo SAA/NC in comparison with other representative catalysts, listed in Tab. S2.

Table S1. Structural parameters extracted from Pt L_3-edge EXAFS fitting. (S_0^2=0.84).

Sample	Path	CN	R(Å)	$\sigma^2(10^{-3}Å^2)$	ΔE_0(eV)	R factor
PtCo SAA/NC	Pt-Co	1.0	2.59	4.7	2.2	0.012
	Pt-N	2.7	1.88	4.3		

S_0^2 is the amplitude reduction factor; CN is the coordination number; R is interatomic distance (the bond length between Ni central atoms and surrounding coordination atoms); σ^2 is Debye-Waller factor (a measure of thermal and static disorder in absorber-scatterer distances); ΔE_0 is edge-energy shift (the difference between the zero kinetic energy value of the sample and that of the theoretical model). R factor is used to value the goodness of the fitting.

Table S2. Structural parameters extracted from Co K-edge EXAFS fitting. ($S0^2$=0.84).

Sample	Path	CN	R(Å)	$\sigma^2(10^{-3}Å^2)$	ΔE_0(eV)	R factor
Co NPs/NC	Co-Co	9.8	2.56	7.9	2.5	0.010

S_0^2 is the amplitude reduction factor; CN is the coordination number; R is interatomic distance (the bond length between Ni central atoms and surrounding coordination atoms); σ^2 is Debye-Waller factor (a measure of thermal and static disorder in absorber-scatterer distances); ΔE_0 is edge-energy shift (the difference between the zero kinetic energy value of the sample and that of the theoretical model). R factor is used to value the goodness of the fitting.

Table S3. Summary of various Co based catalysts in acidic condition at 10 mA cm^{-2}.

Material	Electrolyte	Overpotential /mV	Tafel slope/(mV dec^{-1})	Ref.
PtCo SAA/NC	0.5 M H_2SO_4	52	42	This Work
Co Nps/NC	0.5 M H_2SO_4	126	116	This Work
PtCo NPs/NC	0.5 M H_2SO_4	73	68	This Work
Co-N_4C_4	0.5 M H_2SO_4	175	80	1
Co-3C_1N	0.5 M H_2SO_4	138	55	2
Co-NG	0.5 M H_2SO_4	147	82	3
CoP/CC	0.5 M H_2SO_4	67	51	4
Co_1/PCN	0.5 M H_2SO_4	151	74	5
CoNC-Cl	0.5 M H_2SO_4	130	41	6
Co-900-A	0.5 M H_2SO_4	82	59.32	7
Co^{2+}-Co_9S_8	0.5 M H_2SO_4	86	115.9	8

References

1. H. Fei, J. Dong, C. Wan, Z. Zhao, X. Xu, Z. Lin, Y. Wang, H. Liu, K. Zang, J. Luo, S. Zhao, W. Hu, W. Yan, I. Shakir, Y. Huang and X. Duan, *Adv. Mater.*, 2018, **30**.
2. Z.-L. Wang, X.-F. Hao, Z. Jiang, X.-P. Sun, D. Xu, J. Wang, H.-X. Zhong, F.-L. Meng and X.-B. Zhang, *J. Am. Chem. Soc.*, 2015, **137**, 15070-15073.
3. H. Fei, J. Dong, M. J. Arellano-Jiménez, G. Ye, N. Dong Kim, E. L. G. Samuel, Z. Peng, Z. Zhu, F. Qin, J. Bao, M. J. Yacaman, P. M. Ajayan, D. Chen and J. M. Tour, *Nat. Commun.*, 2015, **6**.
4. J. Tian, Q. Liu, A. M. Asiri and X. Sun, *J. Am. Chem. Soc.*, 2014, **136**, 7587-7590.
5. L. Cao, Q. Luo, W. Liu, Y. Lin, X. Liu, Y. Cao, W. Zhang, Y. Wu, J. Yang, T. Yao and S. Wei, *Nat. Catal.*, 2018, **2**, 134-141.
6. G. Wan, C. Yang, W. Zhao, Q. Li, N. Wang, T. Li, H. Zhou, H. Chen and J. Shi, *Adv. Mater.* 2017, **29**.
7. R. Ding, Y. Chen, X. Li, Z. Rui, K. Hua, Y. Wu, X. Duan, X. Wang, J. Li and J. Liu, *Small*, 2021, **18**.
8. B. Tian, W. Kolodziejczyk, J. Saloni, P. Cheah, J. Qu, F. Han, D. Cao, X. Zhu and Y. Zhao, *J. Mater. Chem. A*, 2022, **10**, 3522-3530.